Journal of Controlled Release 210 (2015) 169–178

Contents lists available at ScienceDirect

Journal of Controlled Release

journal homepage: www.elsevier.com/locate/jconrel

Controlled delivery of a metabolic modulator promotes regulatory T cells and restrains autoimmunity

Joshua M. Gammon [a], Lisa H. Tostanoski [a], Arjun R. Adapa [a], Yu-Chieh Chiu [a], Christopher M. Jewell [a,b,c,*]

[a] Fischell Department of Bioengineering, University of Maryland, College Park, MD, United States
[b] Department of Microbiology and Immunology, University of Maryland Medical School, Baltimore, MD, United States
[c] Marlene and Stewart Greenebaum Cancer Center, Baltimore, MD, United States

ARTICLE INFO

Article history:
Received 9 March 2015
Received in revised form 16 May 2015
Accepted 18 May 2015
Available online 19 May 2015

Keywords:
Nanoparticle
Tolerance
Biomaterial
Immunotherapy
Metabolism
Autoimmunity
Immunology
Vaccine

ABSTRACT

Autoimmune disorders occur when the immune system abnormally recognizes and attacks self-molecules. Dendritic cells (DCs) play a powerful role in initiating adaptive immune response, and are therefore a recent target for autoimmune therapies. *N*-Phenyl-7-(hydroxyimino)cyclopropa[*b*]chromen-1a-carboxamide (PHCCC), a small molecule glutamate receptor enhancer, alters how DCs metabolize glutamate, skewing cytokine secretion to bias T cell function. These effects provide protection in mouse models of multiple sclerosis (MS) by polarizing T cells away from inflammatory T_H17 cells and toward regulatory T cells (T_{REG}) when mice receive daily systemic injections of PHCCC. However, frequent, continued treatment is required to generate and maintain therapeutic benefits. Thus, the use of PHCCC is limited by poor solubility, the need for frequent dosing, and cell toxicity. We hypothesized that controlled release of PHCCC from degradable nanoparticles (NPs) might address these challenges by altering DC function to maintain efficacy with reduced treatment frequency and toxicity. This idea could serve as a new strategy for harnessing biomaterials to polarize immune function through controlled delivery of metabolic modulators. PHCCC was readily encapsulated in nanoparticles, with controlled release of 89% of drug into media over three days. Culture of primary DCs or DC and T cell co-cultures with PHCCC NPs reduced DC activation and secretion of pro-inflammatory cytokines, while shifting T cells away from T_H17 and toward T_{REG} phenotypes. Importantly, PHCCC delivered to cells in NPs was 36-fold less toxic compared with soluble PHCCC. Treatment of mice with PHCCC NPs every three days delayed disease onset and decreased disease severity compared with mice treated with soluble drug at the same dose and frequency. These results highlight the potential to promote tolerance through controlled delivery of metabolic modulators that alter DC signaling to polarize T cells, and suggest future gains that could be realized by engineering materials that provide longer term release.

1. Introduction

Polymeric nanoparticles (NPs) are ubiquitous in nanotechnology owing in part to the ability of these materials to encapsulate and control the release of hydrophobic, small molecule drugs [1]. Recently, this approach has become of great interest for polarizing immune cells (e.g., T cells) toward functions tailored for specific vaccine, cancer, and immunotherapy applications [2–4]. Here we investigated a new idea for driving this polarization through controlled release of small molecules that control immune cell metabolism to promote tolerance and restrain autoimmunity. In these studies we employed a well-understood NP platform to test if controlled release of these drugs would alter dendritic cell (DC) function, promote regulatory T cells, and more effectively control disease in mouse models of autoimmunity with less frequent dosing and reduced toxicity.

Autoimmune disease occurs when the adaptive immune system recognizes and attacks self molecules. Multiple sclerosis (MS) is an autoimmune disease in which myelin — a protein that insulates neurons — is attacked, causing inflammation and neurodegeneration in the central nervous system (CNS). Some of the key effector cell populations that drive these detrimental effects are inflammatory subsets of myelin-reactive $CD4^+$ T cells [5–7]. Further, high levels of glutamate are present in the central nervous system during MS, leading to a state of excitotoxicity that exacerbates inflammation and depletes oligodendrocytes — the cells responsible for remyelinating neurons [8,9]. The metabotropic glutamate receptor (mGluR) family helps control these effects, resulting in inflammation or protection against excitotoxicity, depending on the relative presence and activity of each mGluR receptor in the CNS during disease [8–11]. In particular, metabolism of glutamate

* Corresponding author at: Fischell Department of Bioengineering, 2212 Jeong H. Kim Engineering Building, College Park, MD 20742, United States.
E-mail address: cmjewell@umd.edu (C.M. Jewell).
URL: http://www.jewell.umd.edu (C.M. Jewell).

http://dx.doi.org/10.1016/j.jconrel.2015.05.277

through mGluR4 reduces *N*-Methyl-D-aspartate toxicity in cortical neurons and kainate mediated toxicity in oligodendrocytes [11,12].

In addition to serving as a neurotransmitter, glutamate also functions as an immunomodulator by interacting with glutamate receptors expressed on the surface of DCs or other immune cells [13]. DCs play a key role in initiating adaptive immunity by processing and presenting exogenous antigens, or in the case of autoimmune diseases such as MS, self antigens (e.g., myelin). Presentation of these antigens to a cognate T cell drives antigen-specific proliferation and differentiation. The magnitude and type of T cell response is dictated in part by the activation and inflammatory state of DCs during the formation of an immune synapse with a T cell [14]. For example, suppression of DC activation can induce secretion of regulatory cytokines that diminish T cell expansion and shift the phenotypes toward regulatory T cells (T_{REG}) and away from inflammatory T cells (e.g., T_H17) [15–17].

During inflammation, DCs release glutamate that regulates T cell activation and proliferation by binding glutamate receptors on DCs and T cells [13,18,19]. The identity and abundance of the mGluRs that are bound by glutamate alters cAMP levels, modulating the balance of inflammatory and regulatory cytokines that direct the resulting immune response. This mechanism has stimulated interest in controlling glutamate receptor signaling as one route to regulate immune cell function in new therapies for MS [19–21]. The Di Marco group recently demonstrated that mGluR4 is expressed at high levels on DCs and exerts an immunoregulatory function by showing that DCs with defective mGluR4 signaling preferentially polarize T cells to inflammatory T_H17 phenotypes. This work further revealed that *N*-Phenyl-7-(hydroxyimino)cyclopropa[*b*]chromen-1a-carboxamide (PHCCC), a small molecule positive allosteric modulator of mGluR4, can bias T cell function toward tolerance during autoimmunity in mice [12,19]. Prophylactic treatment of mice with PHCCC during Experimental Autoimmune Encephalomyelitis (EAE) – a mouse model of MS – inhibited clinical symptoms of neuroinflammation by inducing regulatory cytokine profiles in DCs that promoted T_{REGS} and reduced T_H17 cells [10]. However, the use of PHCCC is hindered by poor solubility and a short half-life [22], with neurological symptoms and paralysis returning within one day after daily systemic injections were stopped [19].

To address these challenges, we hypothesized that controlled release of PHCCC might maintain or improve efficacy while offering less frequent dosing and reduced toxicity. Our studies revealed that NPs were readily endocytosed by DCs and reduced inflammatory cytokines. Strikingly, these effects were achieved with a 36-fold decrease in toxicity compared to soluble PHCCC. During co-culture with myelin-specific T cells, DCs treated with PHCCC NPs reduced T_H17 cells and increased T_{REGS}, while reducing inflammatory cytokines. Treatment of mice with PHCCC NPs every three days delayed disease onset and decreased severity compared with soluble drug. These results demonstrate a biomaterial-based approach to promote tolerance by harnessing controlled release for modulation of DC metabolic function.

2. Materials and methods

2.1. Materials

PHCCC was purchased from Tocris Bioscience. Poly(lactide-co-glycolide) (PLGA, 30,000–60,000 MW, 50:50 lactide:glycolide), polyvinyl alcohol (PVA) (MW 89,000–98,000), acetone, wheat germ agglutinin Texas Red conjugate, ethylenediaminetetraacetic acid (EDTA), sesame oil, and bovine serum albumin (BSA) were purchased from Sigma. Dimethyl-sulfoxide (DMSO) was purchased from Fisher scientific. Myelin oligodendrocyte glycoprotein ($MOG_{35–55}$) and SIINFEKL peptides were synthesized by Genscript. Antibodies for flow cytometry were purchased from BD biosciences and included CD11c APC-Cy7, CD40 PE, CD86 PE-Cy7, CD80 APC, CD4 APC-Cy7, CD4 FITC, RORγ PE and FoxP3 Alexa Fluor 647. Anti-mouse H-2 kb bound to SIINFEKL PE-Cy7 was purchased from Biolegend. 4′,6-diamidino-2-phenylindole (DAPI), DiO, lipopolysaccharide (LPS) and Hoechst nuclear stain were purchased from Invitrogen. DC and T cell culture media was RPMI 1640 base media (Lonza) supplemented with 10% fetal bovine serum (Corning), 100 μg/100 U penicillin–streptomycin (Lonza), 10 mM HEPES (Thermo Scientific), 2 mM L-glutamine (Lonza), 55 μM beta-mercaptoethanol (MP Biomedical), and non-essential amino acids (1×, Thermo Scientific).

2.2. Cells and mice

For in vitro studies, DCs were magnetically isolated from the spleens of naïve, female, C57BL/6J mice (4 weeks) using CD11c positive selection microbeads (Miltenyi). $CD4^+$ T cells were isolated from the spleens of transgenic female, C57BL/6-Tg(Tcra2D2,Tcrb2D2)1Kuch/J (2D2) mice using negative magnetic cell isolation (Stemcell Technologies). $CD4^+$ T cell receptors in this strain recognize and respond to MOG presented via the MHC-II complex [23]. EAE was induced in 10 week old, female, C57BL/6J mice as described below. All animal care and experiments were carried out using protocols approved and overseen by the University of Maryland IACUC committee.

2.3. Particle synthesis and characterization

PLGA NPs encapsulating PHCCC were synthesized by nanoprecipitation. The solvent phase was prepared by dissolving 25 mg of PLGA in 1.5 mL acetone. For samples loaded with PHCCC, this polymer solution was transferred to a vial containing the appropriate mass of dried PHCCC. For samples loaded instead with DiO, 5 μL of 1 μM DiO solution was added to the polymer solution. The non-solvent phase consisted of 20 mL deionized water with 0–2% PVA. The solvent phase was then uniformly injected through a 31 g needle under the surface of the non-solvent phase while mixing with a magnetic stir bar. The solvent was evaporated for 3 h, leaving a suspension of stabilized NPs. The suspension was poured through a 40 μm cell strainer then centrifuged for 75 min at 4 °C at 3000 g. The supernatant was decanted and the NPs were resuspended in deionized water.

To measure PHCCC encapsulation, NPs were dried and dissolved in DMSO. The absorbance was then measured at 300 nm on a UV–VIS spectrophotometer and corrected by subtracting the absorbance value measured for empty NPs dissolved at the same mass concentration in DMSO. Absorbance values were compared to a PHCCC standard curve to determine a mass concentration. Particle size distributions were measured by laser diffraction using a Horiba Partica LA 950V2.

To measure release kinetics, known concentrations of PHCCC NPs were incubated at 37 °C in RPMI 1640 media under sink conditions to eliminate release effects arising from saturated drug solution. At each interval PHCCC NPs were centrifuged at 18,000 *g* for 5 min, and PHCCC concentration in the supernatants was determined by UV–VIS spectrophotometry as above. Particles were then resuspended in media and returned to incubation at 37 °C. The cumulative PHCCC released was calculated at each time and normalized to the total loading to calculate the percent of PHCCC released.

2.4. Flow cytometry

Flow cytometry was carried out on a FACSCantoII flow cytometer (BD Biosciences). Cells were first detached from the 96 well culture plates with cold 10 mM EDTA, then washed with 1% BSA in PBS. Cells were blocked by incubation at room temperature in 20 μg/mL rat anti-mouse CD16/CD32 (BD Biosciences) for 10 min. Blocked cells were stained with antibodies diluted in PBS + 1% BSA for 20 min at room temperature protected from light. Cells were then washed twice with PBS + 1% BSA and either resuspended in PBS + 1% BSA (with or without 5 μg/mL DAPI) for immediate analysis, or fixed and stained for intracellular markers. For intracellular staining, cells were resuspended in

FoxP3 fixation/permeabilization buffer (Ebioscience), and incubated for 2 h at 4 °C in the dark. Cells were then washed twice with FoxP3 permeabilization buffer (Ebioscience) and resuspended in antibodies against the appropriate intracellular markers diluted in FoxP3 permeabilization buffer. Cells were incubated at 4 ° C for 40 min in the dark. Stained cells were washed twice with FoxP3 permeabilization buffer then resuspended in PBS + 1% BSA for analysis.

2.5. Particle uptake and toxicity studies

Isolated DCs were plated in flat bottom 96 well plates and incubated in media with the specified concentrations of DiO NPs for 90 min. Cells were washed with PBS to remove free NPs, and then detached using cold, 10 mM EDTA. Detached cells were washed with cold PBS + 1% BSA, then resuspended in DAPI (5 μg/mL) in PBS + 1% BSA. DCs were analyzed by flow cytometry to determine the percentages of cells positive for DiO (particles). For analysis of particle uptake by microscopy, splenic $CD11c^+$ DCs were plated in 35 mm dishes and incubated in media with DiO NPs for 90 min. Cells were washed with PBS to remove free NPs, then fixed with 4% paraformaldehyde for 15 min at 37 °C. Cell membranes were stained at room temperature in the dark for 10 min with 5 μg/mL wheat germ agglutinin Texas Red conjugate in PBS. The cells were then washed with PBS, labeled with Hoechst nuclear stain diluted to 2 μg/mL in PBS. Cells were imaged using a Leica SP5 X laser scanning confocal microscope with a 63× objective.

To analyze toxicity of soluble PHCCC or PHCCC delivered in NP format, $CD11c^+$ cells isolated from splenocytes (1×10^5 cells/well) were stimulated with LPS (1 μg/mL) and treated with equivalent concentrations of PHCCC delivered in soluble or NP format. After 18 h toxicity was analyzed by flow cytometry by staining with DAPI and quantifying the percentage of $DAPI^-$ events. Relative viability was calculated by normalizing the percent of viable cells to the value of the untreated LPS stimulated control. The fold-decrease in toxicity was calculated by dividing the relative viability of cells treated with PHCCC NPs by the value for cells treated with soluble PHCCC at 400 μM.

2.6. DC activation, antigen presentation and cytokine secretion

For analysis of DC activation and cytokine secretion, $CD11c^+$ cells isolated from splenocytes (1×10^5 cells/well) were stimulated with LPS (1 μg/mL) and left untreated or treated with soluble PHCCC (40 μM), PHCCC NPs, or empty NPs using equivalent particle masses. For soluble PHCCC controls, PHCCC was dissolved in DMSO to 20 mM then diluted to a final concentration of 40 μM in media. DMSO concentration in the well was 0.2% (v/v). After 18, 44 and 68 h, cells and cell culture supernatants were collected. IL-6 and IL-10 concentrations in the supernatants were determined by ELISAs (BD Biosciences). The collected cell pellets were stained as above for viability ($DAPI^-$), CD11c (APC-Cy7) and activation/costimulatory markers (i.e., FITC I-A/I-E, PE CD40, PE-Cy7 CD86, APC CD80). Cells were gated under $DAPI^-$/$CD11c^+$ negative events.

For analysis of DC antigen presentation, DCs stimulated with LPS were treated with PHCCC, PHCCC NPs, and empty NPs as in DC activation studies. After 18 h, cells were incubated for 2 h with SIINFEKL peptide (5 μg/mL), or with $MOG_{35–55}$ (5 μg/mL) as an irrelevant peptide control. Cells were then stained for presentation of SIINFEKL via the H-2 kb complex using an antibody which binds SIINFEKL when presented in H-2 kb. Cells were gated under $CD11c^+$/$DAPI^-$.

2.7. Co-culture of DCs with transgenic 2D2 T cells

Isolated DCs (1×10^5 cells/well) were stimulated with LPS (1 μg/mL) and MOG (10 μg/mL) and treated with soluble PHCCC (40 μM), PHCCC NPs, or empty NPs. After 18 h, splenic $CD4^+$ T cells isolated from 2D2 mice (3×10^5 cells/well) were added to the DC culture. After an additional 2 days, supernatants were collected and IFNγ concentrations were measured by ELISA (BD Bioscience). Cells from these cultures were stained for CD4 and CD25 surface markers, along with FoxP3 and RORγ transcription factors as markers for T_{REGS} ($CD4^+$/$CD25^+$/$FoxP3^+$) and inflammatory T_H17 cells ($CD4^+$/$ROR\gamma^+$), respectively.

2.8. T cell proliferation studies

For proliferation studies, splenic $CD4^+$ T cells isolated from 2D2 mice were incubated with carboxyfluorescein succinimidyl ester (CSFE) before addition to DCs treated with LPS, peptide, and particles as above. The T cells were labeled by resuspension in media at 50×10^6 cells/mL then incubation in CSFE at a final concentration of 5 μM for 5 min at room temperature. Cells were washed four times with media, then added to the DC cultures. Cells were collected 72 h later and analyzed by flow cytometry to determine the extent of T cell proliferation (i.e., CSFE levels among $CD4^+$/$DAPI^-$ cells). Analysis was performed using FlowJo software (Treestar).

2.9. EAE induction and treatment with PHCCC NPs

EAE was induced in 10 week old C57BL/6 mice as previously described [24,25]. Briefly, mice were immunized with two subcutaneous (*s.c.*) injections of emulsions prepared from complete Freund's adjuvant (CFA) and 100 μg of $MOG_{35–55}$ in killed mycobacterium tuberculosis H37Ra (200–500 μg). Subsequently, 200 ng of pertussis toxin in 100 μL of PBS was injected intra-peritoneal (i.p.) on the day of immunization and again the following day.

Soluble PHCCC, PHCCC NPs (each 3 mg/kg with respect to drug dose) were administered s.c. at the tailbase every 3 days or every 5 days beginning on the day of EAE induction (day 0). For soluble treatment, PHCCC was dissolved in sesame oil [19] and PHCCC NPs were suspended in deionized water. Empty NPs at the same mass as the PHCCC NP treatments were included as controls. Mice were weighed and scored daily for signs of disease using an accepted clinical pathology scoring scale: 0, no symptoms; 1, limpness in entire tail; 2 weakness in hind legs; 3, paralysis of hind legs or paralysis of one front leg and one hind leg; 4, moribund. Mice were euthanized according to defined endpoints if a score of 4.5 was reached, upon a score of 4.0 for 2 days, or upon 25% weight loss (with respect to initial weight).

3. Results

3.1. PHCCC is encapsulated into nanoparticles at high levels and released over three days

Toward the goal of maintaining drug function while reducing toxicity and frequency of treatment, we first developed protocols to synthesize PHCCC-loaded NPs by nanoprecipitation. PHCCC was successfully encapsulated in NPs at high levels, with PHCCC loading levels correlated with increasing ratios of drug to polymer input. Loading was optimal at a drug:polymer input ratio of 0.2, which resulted in a drug loading level of 73.2 ± 25.9 μg of PHCCC per mg of NPs (Table 1). Further increasing the drug to polymer ratio to 0.4 or higher did not result in any further

Table 1
Properties of PHCCC NPs synthesized with different input ratios of PHCCC to PLGA.

PHCCC:polymer input ratio	PHCCC input	Polymer input	Loading level	Diameter
(mg)	(mg)	(mg)	(μg PHCCC/mg particle)	(nm)
0	0	25	N/A	125.2 ± 60.2
0.04	1	25	25.4 ± 12.2	132.9 ± 36.4
0.12	3	25	44.7 ± 13.3	185.9 ± 33.7
0.2	5	25	73.2 ± 25.9	148.5 ± 47.1
0.4	10	25	78.3 ± 12.9	114.4 ± 42.2

increase in loading. NPs exhibited relatively uniform size distributions, with mean diameters ranging from 114–186 nm depending on the drug to polymer ratio (Fig. 1A and B). To examine the release kinetics of PHCCC from NPs, particles were incubated in media at 37 °C. PHCCC NPs released 66.3% of drug over the first 4 h, followed by a slower release rate that accounted for release of 89.1% of total encapsulated drug after 72 h (Fig. 1C).

3.2. NPs are efficiently internalized by DCs with reduced toxicity compared to soluble PHCCC

To test the ability of DCs to internalize NPs, fluorescently-labeled empty NPs were incubated with $CD11c^+$ splenic DCs for 90 min. Flow cytometry analysis of these samples revealed a dose dependent uptake of NPs with up to 58.4 ± 2.8% of live, $CD11c^+$ cells positive for NPs (Fig. 1D). Visualization of cells by confocal microscopy confirmed these results, showing punctate NPs distributed throughout the cytosolic regions of DCs (Fig. 1E, green signal). To assess the toxicity of PHCCC on immune cells, we stimulated DCs with LPS, along with varying doses of PHCCC in soluble form or loaded in NPs. After 18 h, only 2.2% of cells treated with LPS and soluble PHCCC remained viable relative to cells treated with LPS alone (Fig. 1F). Strikingly, 83.6% of DCs remained viable following treatment with LPS and an equivalent concentration of PHCCC in NP form, representing a 36-fold reduction in toxicity (Fig. 1F).

3.3. PHCCC NPs alter DC cytokine secretion profiles

To determine what range of drug input levels in NPs would alter DC function, DCs were stimulated with LPS and incubated with a fixed dose of PHCCC loaded in NPs that were prepared using different drug:polymer ratios (Fig. 2, green bars). Empty NP (Fig. 2, gray bars) controls were prepared at the same mass of NPs (i.e., polymer) used for PHCCC NPs to confirm that the effect of PHCCC NPs was attributable to encapsulated PHCCC. The levels of IL-6 and IL-10 secretion were then measured in the supernatants to determine if PHCCC NPs reduced the inflammatory effects caused by LPS treatment. IL-6 levels generally increased over the 3 day incubation, but at each time point, DCs treated with LPS and a fixed drug dose loaded in PHCCC NPs, caused a significant reduction in IL-6 secretion compared with cells treated with LPS only (Fig. 2A–C). These reductions were not as large as those observed in samples treated with soluble PHCCC. In contrast, empty particles generally did not cause a significant change in IL-6 level. However, at empty particle masses equivalent to those used for the lowest drug:polymer ratio (i.e., highest polymer mass), empty NP controls had a modest effect on IL-6 secretion. PHCCC also decreased IL-10 secretion, but the kinetics of this reduction after treatment with soluble PHCCC or PHCCC NPs was delayed compared with the timeline observed for IL-6 (Fig. 2D–F). The effects of PHCCC NPs were evident at 44 h and 68 h, but not at the earlier time point of 18 h where no differences were observed between empty NPs and PHCCC NPs (Fig. 2D–F). Control studies with the same dilute levels of DMSO (0.2%) used to solubilize free PHCCC confirmed this vehicle had no effect on toxicity, cytokine levels, or activation, compared with wells treated with media or LPS without DMSO.

A further optimization study was performed by varying the stabilizer (i.e., PVA) concentration for NPs prepared at a drug:polymer ratio of 0.2 (Fig. S1). This ratio was selected since PHCCC loading was most efficient using this drug input ratio, and minimal background effects were observed from empty particles. In the stabilizer studies, the effect of empty NPs on cytokine secretion was minimized at a PVA concentration of 2% (Fig. S1). Therefore particles synthesized using these two parameters were chosen for all subsequent studies.

Using the optimized particle formulation, we next identified a dosing range where PHCCC NPs modulate DC function by stimulating DCs with LPS and treating with a range of PHCCC NP doses. For IL-6, a dose dependent response was observed at each time point, with PHCCC NPs at higher concentrations causing larger reduction in IL-6 secretion

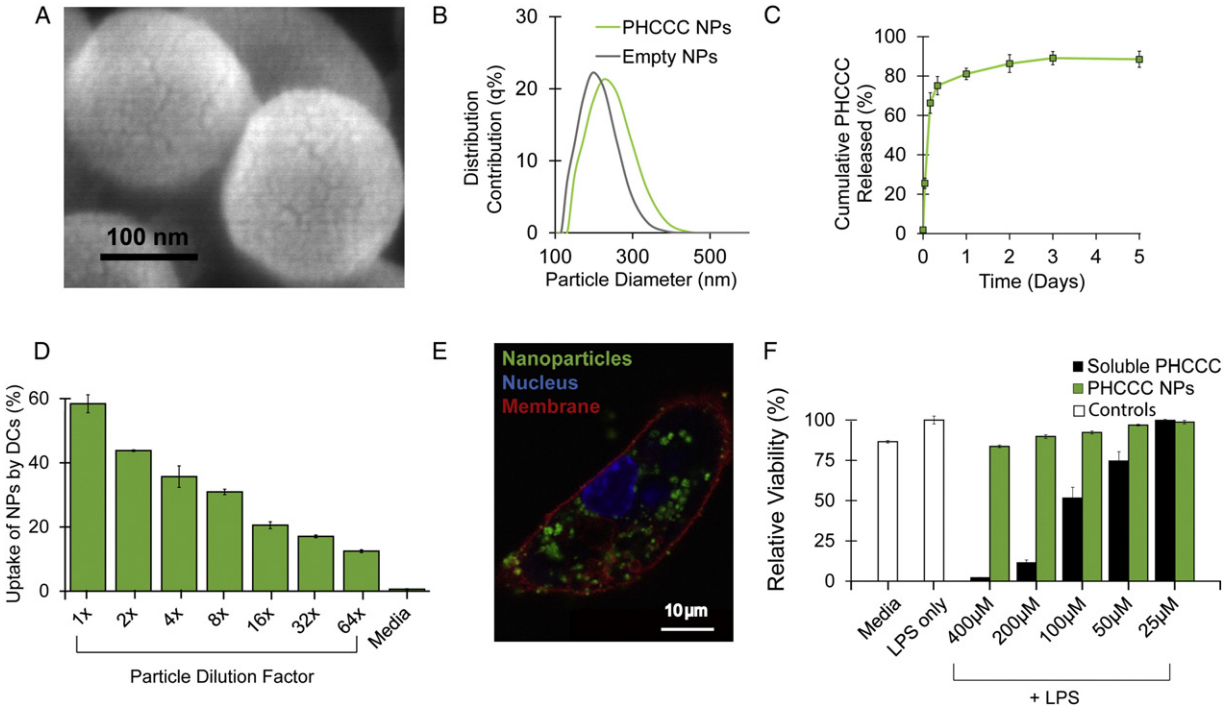

Fig. 1. NPs synthesized by nanoprecipitation are internalized by DCs and eliminate toxicity observed from soluble PHCCC. (A) SEM image of PHCCC NPs. (B) Histogram showing size distribution of PHCCC NPs synthesized with 2% PVA and a drug to polymer ratio of 0.2. (C) In vitro release kinetics of PHCCC NPs. (D) Primary splenic DCs were incubated for 90 min with fluorescent NPs, and the percent of DCs positive for NP uptake was quantified by flow cytometry. (E) Confocal microscopy image of DCs treated as in (D), demonstrating colocalization of NPs (green) within cells. DCs were stained with a Texas Red wheat germ agglutinin conjugate (red) and Hoechst nuclear stain (blue). (F) Primary splenic DCs were stimulated with LPS (1 μg/mL) and treated with PHCCC in soluble or NP form. Viability relative to LPS stimulated cells was quantified by DAPI staining and analysis by flow cytometry. All data were collected in triplicate and are representative of 3 similar experiments.

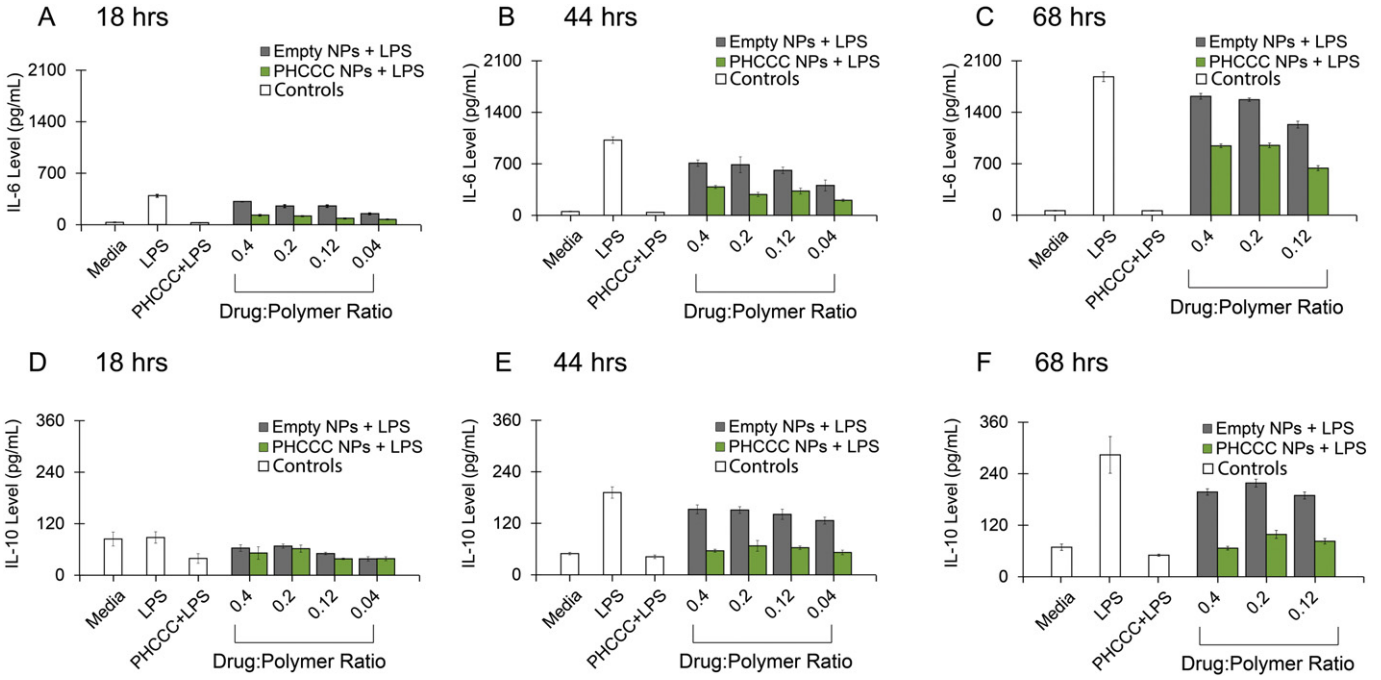

Fig. 2. Impact of PHCCC loading in NPs on DC cytokine secretion. CD11c^{+} cells isolated from spleens were stimulated with LPS (1 μg/mL) and treated with soluble PHCCC or PHCCC NPs (100 μM with respect to drug) synthesized by fixing polymer mass and varying drug input (drug:polymer ratio). Cells treated with equivalent masses of empty NPs were also included as controls. Supernatants were collected and the concentrations of IL-6 (A–C) and IL-10 (D–F) were measured by ELISA at 18 h (A, D), 44 h (B, E), and 68 h (C, F). Samples were prepared in triplicate and data are representative of results from at least 3 similar experiments.

(Fig. 3A–C). A similar trend was observed at 44 h and 68 h for IL-10, but was less clear at the 18 h time point (Fig. 3D–F). Empty NP controls did not significantly suppress IL-6, but caused a modest decrease in IL-10 levels at 44 h and 68 h compared with LPS. However, at all three time points PHCCC NPs significantly decreased cytokine secretion compared to empty NPs.

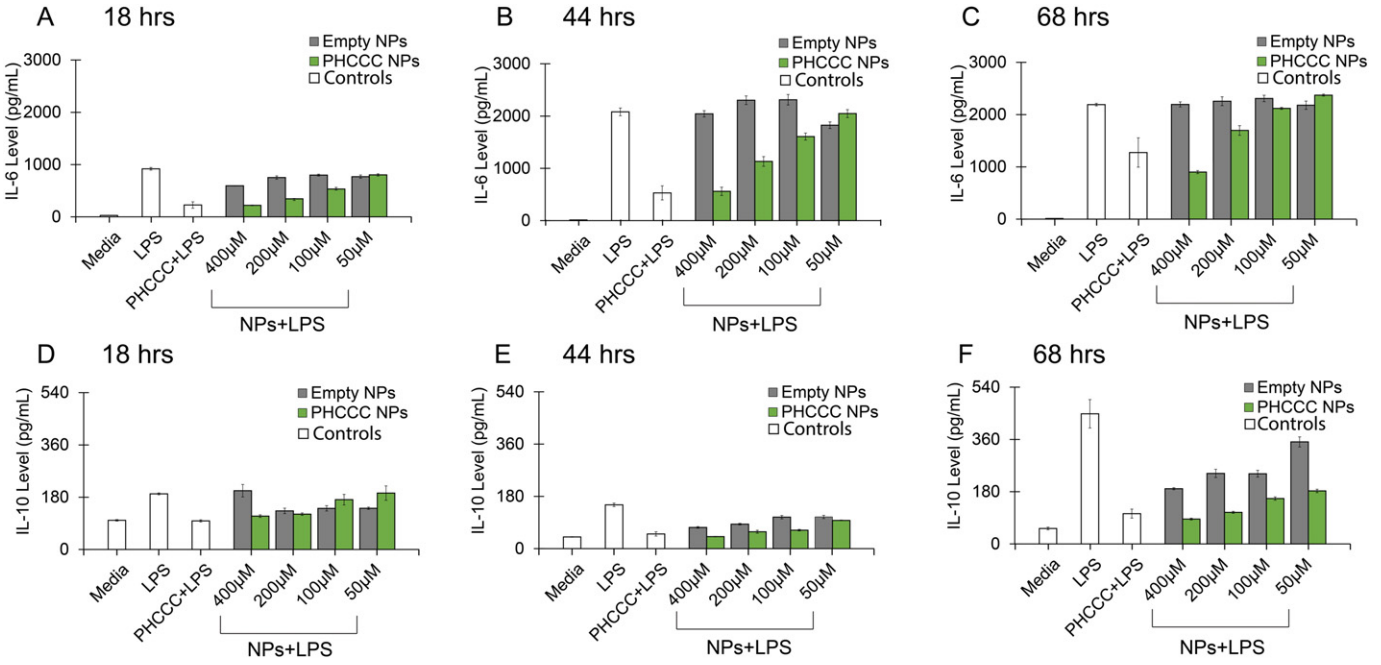

Fig. 3. PHCCC NPs alter cytokine secretion by DCs in a dose dependent manner. CD11c^{+} cells isolated from spleens stimulated with LPS (1 μg/mL) were treated with soluble PHCCC, PHCCC NPs at decreasing doses, or equivalent masses of empty NPs. Supernatants were collected and the concentrations of IL-6 (A–C) and IL-10 (D–F) were measured by ELISA at 18 h (A, D), 44 h (B, E), and 68 h (C, F). Samples were prepared in triplicate and data are representative of results from at least 3 similar experiments.

3.4. PHCCC NPs decrease DC activation and antigen presentation

T cell proliferation and phenotype (e.g., T_H17 vs. T_{REG}) are dependent on the levels and balance of antigen and co-stimulatory signals presented by DCs. To test the hypothesis that PHCCC NPs would decrease stimulatory cues presented by DCs, DCs were stimulated with LPS and left untreated or treated with PHCCC in soluble or NP form. After 18 h, flow cytometry was used to assess CD40, CD80, and CD86 expression, as well as loading and presentation of a common antigenic peptide by the MHC-I pathway. As shown in Fig. 4A–C (green bars), PHCCC NPs significantly decreased CD40, CD80 and CD86 expression on DCs relative to DCs cultured only with LPS. These effects were dose dependent and were comparable to the reduction caused by soluble PHCCC. Compared with LPS-treated positive controls, empty NPs did not significantly alter DC activation at any concentration (Fig. 4A–C, gray bars), though for CD40, a slight reduction in expression was observed at the highest doses.

To assess the impact of PHCCC NPs on antigen presentation, DCs were incubated with LPS, soluble PHCCC or PHCCC NPs, and SIINFEKL peptide — a common model antigen derived from ovalbumin. After 20 h, cells were stained with an antibody that binds SIINFEKL only when presented in MHC-I (H-2 kb). While 81.3 ± 0.7% of cells treated with LPS and SIINFEKL presented this antigen via MHC-I (Fig. 4D), treatment with PHCCC NPs reduced SIINFEKL presentation to 30.3% ± 3.0%, depending on NP dose (Fig. 4D, green bars). The magnitude of this reduction was significant compared with cells lacking PHCCC treatments, but less pronounced than the reduction in SIINFEKL presentation observed in cells treated with soluble PHCCC (11.3 ± 4.3%).

3.5. Treatment of DCs with PHCCC NPs restrains T cell expansion and promotes T_{REGS}

To determine if the effects of PHCCC NPs on DC activation and cytokine profiles alter T cell differentiation, we employed a co-culture model in which DCs from wild-type mice were cultured with splenic $CD4^+$ T cells isolated from transgenic 2D2 mice — a strain in which $CD4^+$ T cell receptors are specific for a myelin autoantigen, MOG peptide [23]. DCs were first treated with LPS and MOG, along with soluble PHCCC, PHCCC NPs, or empty NPs at equivalent polymer masses. After 24 h, $CD4^+$ 2D2 splenocytes were added to the culture. 72 h later, cells were collected and T cell proliferation, inflammatory cytokine secretion, and polarization of T_{REG} and T_H17 phenotypes were examined. DCs treated with PHCCC NPs drove proliferation in only 10.8 ± 0.4% of T cells (Figs. 5A and S2, green bars), a striking decrease compared to 55.7 ± 1.9% and 68.4 ± 0.5% observed in DCs treated with soluble PHCCC or those receiving only the stimulants (i.e., MOG + LPS), respectively (Figs. 5A and S2). Attenuation of T cell proliferation was dose dependent, but was significant even at the lowest doses of PHCCC delivered in NP form (25.4 ± 2.2%). Equivalent masses of empty particles did not cause any significant reduction in proliferation compared with cells treated with LPS and MOG. Mean fluorescent intensity (MFI) analysis of these data also confirmed PHCCC NPs significantly reduce proliferation (Fig. 5B).

Treatment of DCs with PHCCC NPs also polarized T cell phenotype, shifting $CD4^+$ T cells away from inflammatory T_H17 phenotypes ($CD4^+/ROR\gamma^+$) and toward T_{REGS} ($CD4^+/CD25^+/FoxP3^+$) (Fig. 5C and D, green). At the highest dose, T_{REG} levels in wells treated with PHCCC NPs were 5.7 ± 0.5%, compared to 3.3 ± 0.7% in samples treated with MOG and LPS, 4.5 ± 0.6% in samples treated with soluble PHCCC, and 3.6 ± 0.7% in cells treated with equal masses of empty particles (Fig. 5C and D). PHCCC NPs also reduced T_H17 levels. In cells treated with MOG and LPS, 82.1 ± 5.3% of $CD4^+$ T cells exhibited a T_H17 phenotype ($CD4^+/ROR\gamma^+$), while soluble PHCCC treatment reduced RORγ frequencies to 67.0 ± 9.9% (Fig. 5E). PHCCC NPs mediated a dose dependent response, with 58.9 ± 1.9% of cells $CD4^+/ROR\gamma^+$ at the highest particle dose (Fig. 5E, green). Supernatants also revealed significant changes in IFNγ production, with PHCCC NPs reducing IFNγ secretion

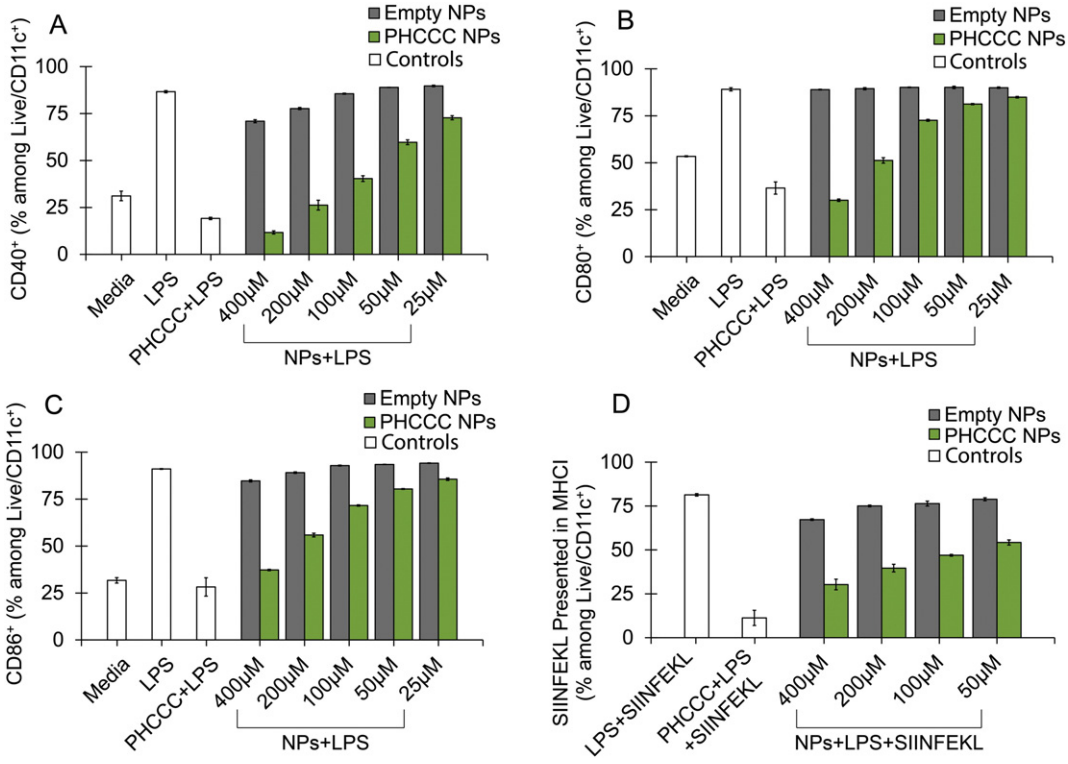

Fig. 4. PHCCC NPs reduce DC activation and antigen presentation. $CD11c^+$ splenocytes were stimulated with LPS (1 μg/mL) and treated with soluble PHCCC, PHCCC NPs at decreasing doses, or equivalent masses of empty NPs. After 18 h cells were collected and the percent of live/$CD11c^+$ cells expressing (A) CD40, (B) CD80, (C) and CD86 were quantified by flow cytometry. (D) $CD11c^+$ splenocytes were stimulated and treated with PHCCC NPs as in (A–C). After 18 h, SIINFEKL peptide (5 μg/mL) was added. Two 2 h later, flow cytometry was used to analyze cells for the percent of live/$CD11c^+$ cells presenting SIINFEKL in H-2 kb. Samples were prepared in triplicate and data are representative of results from at least 3 similar experiments.

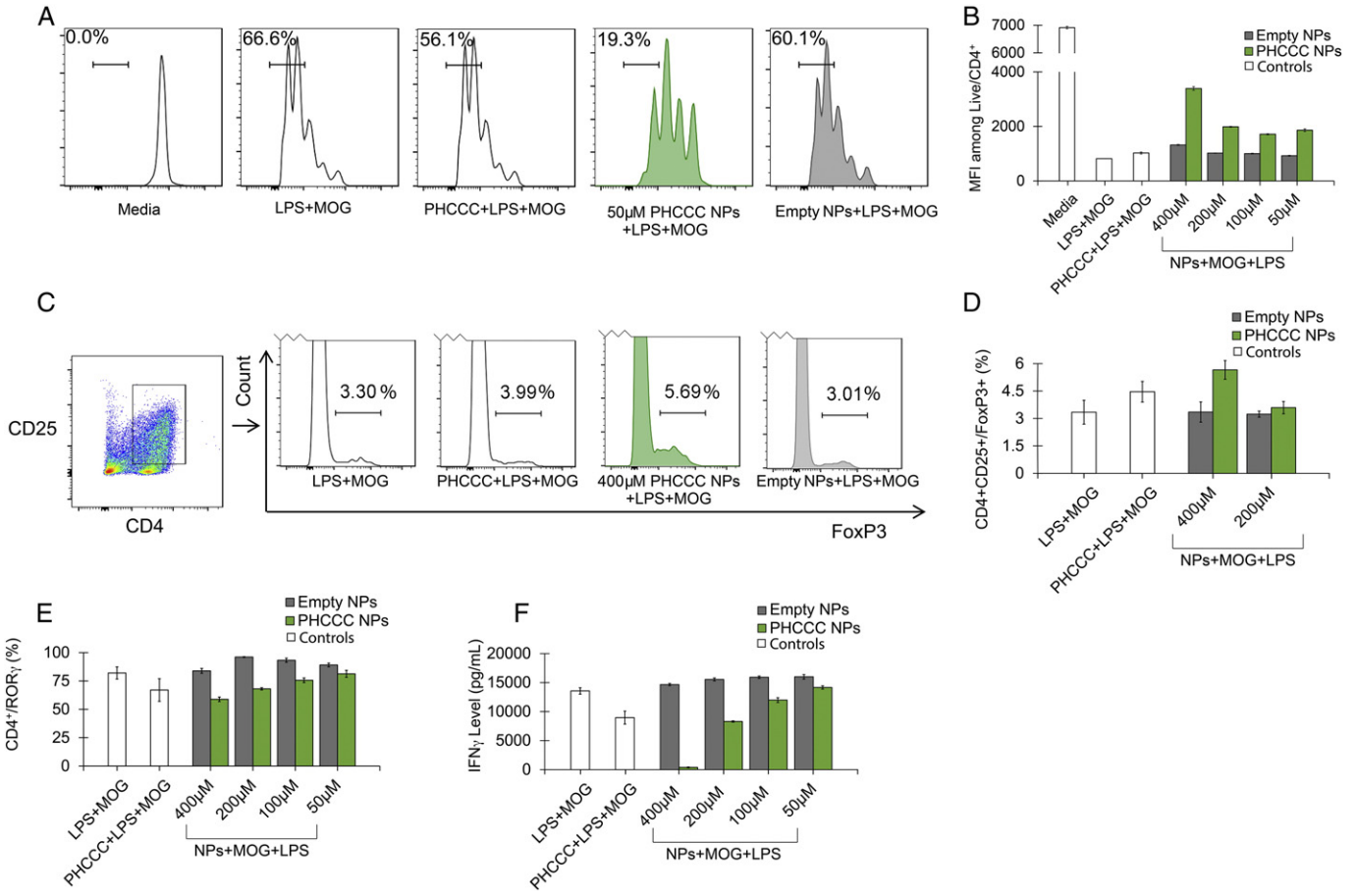

Fig. 5. PHCCC NPs restrain T cell proliferation and inflammatory cytokines, promote T_{REGS}, and reduce T_H17 cells. $CD11c^+$ cells isolated from spleens were stimulated with LPS (1 μg/mL) in the presence of MOG peptide (10 μg/mL), and treated with soluble PHCCC (40 μM), PHCCC NPs at decreasing doses, or equal masses of empty NPs. After 18 h, $CD4^+$ splenocytes from 2D2 mice were added to culture. (A) CSFE dilutions of live/$CD4^+$ T cells from representative co-culture samples and (B) mean fluorescent CSFE intensities (MFI). (C) Gating scheme and histograms of FoxP3 expression among $CD4^+/CD25^+$ cells (i.e., T_{REG}). (D) Frequencies of T_{REGS} measured for each treatment type. (E) Percentages of $CD4^+$ cells expressing RORγ as an indicator of T_H17 cells. (F) IFNγ in supernatants. Samples were prepared in triplicate and results are representative of at least 3 studies.

to 390 ± 77 pg/mL compared to 13600 ± 550 pg/mL after treatment with MOG and LPS, and 8970 ± 1110 pg/mL after treatment with soluble PHCCC (Fig. 5F). These studies confirm PHCCC NPs reduce antigen specific T cell proliferation and inflammatory cytokines, while promoting T_{REGS} and reducing inflammatory (T_H17) phenotypes.

3.6. Treatment with PHCCC NPs every 3 days delays disease and reduces severity in mice with EAE

We next evaluated whether controlled release of PHCCC from NPs could provide a therapeutic benefit during autoimmunity in mice, but with less frequent or less toxic dosing than required for soluble drug. In these studies, mice were induced with EAE, then injected subcutaneously with soluble PHCCC or PHCCC NPs every 5 days starting on the day of EAE induction (day 0) (Fig. 6A). In this study, mice treated with soluble PHCCC or PHCCC NPs exhibited identical disease progression and severity (Fig. 6B–E), and this pathology was identical to mice induced with EAE and treated with empty NPs (Fig. S3). We next tested a regimen in which mice received soluble PHCCC or PHCCC NPs every three days (Fig. 6F). During this regimen, PHCCC NPs caused a statistically significant delay in disease onset (Fig. 6G–I) and decreased disease severity compared to mice treated with soluble PHCCC or empty NPs (Figs. 6J, S3). In groups treated with soluble PHCCC, 100% of mice developed symptoms by day 13, compared to 50% for groups treated with PHCCC NPs (Fig. 6I). Additionally, the maximum mean clinical score over the extent of the study was lower in the PHCCC NP treated group, reaching a value of 2.5 compared to a score of 3.2 for mice receiving soluble PHCCC.

4. Discussion

Several recent immunotherapies have explored controlled release to provide better or more targeted control over the function and phenotype of DCs or T cells. Some of the important drugs that have been tested in this area include mycophenolic acid (MPA) [26], rapamycin [27,28], and 2-(1′H-indole-3′-carbonyl)-thiazole-4-carboxylic acid methyl ester (ITE) [29]. The current study is the first investigation of controlled release of small molecule metabolic enhancers to modulate immune cell function and restrain autoimmunity. Since glutamate is expressed at high, toxic levels during autoinflammation (e.g., during MS), increasing the activity of receptors such as mGluR4 that provide a less toxic metabolic pathway to reduce these levels can help address excitotoxicity and neurodegeneration [11]. Of even greater relevance to our studies, modulating mGluR4 signaling on DCs can decrease the expression of activation markers and alter cytokine secretion profiles to suppress T_H17-mediated inflammation, while driving T cells toward protective T_{REG} phenotypes [10,11]. Thus, PHCCC has the potential to help address both excitotoxicity (by reducing glutamate levels) and inflammation (by redirecting T cell response). Toward this goal, we investigated the ability of controlled release of PHCCC to improve T cell polarization with less toxic, lower frequency dosing.

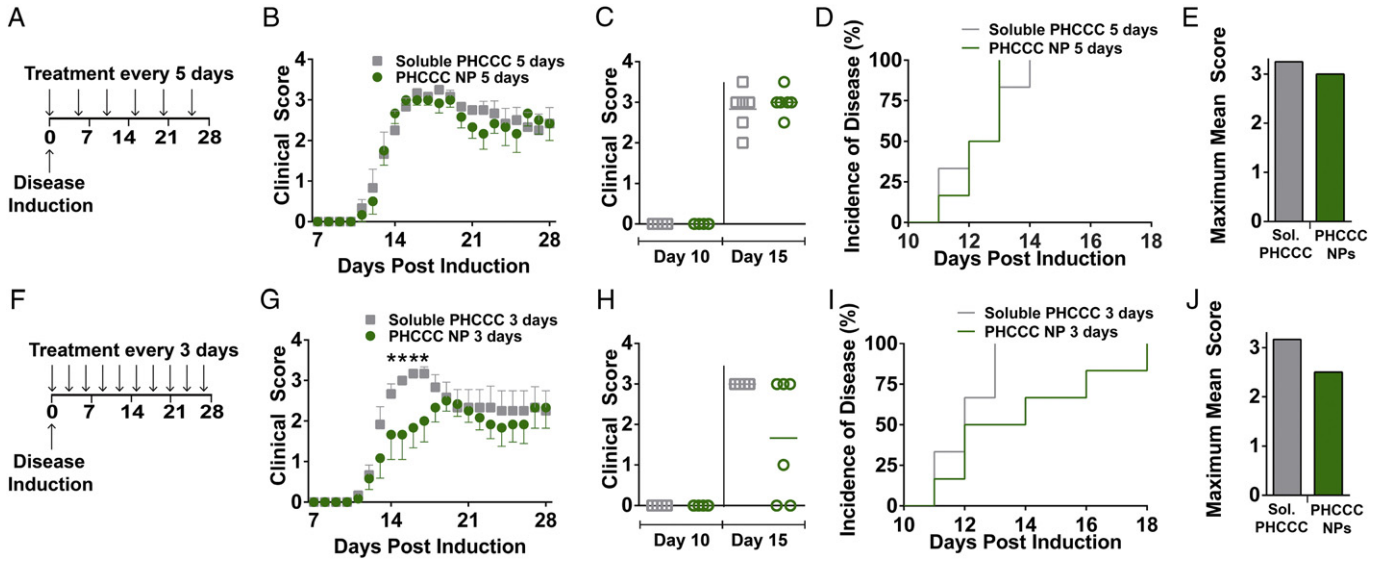

Fig. 6. PHCCC NPs delay the onset of EAE and reduce disease severity. Mice were induced with EAE and treated with 3 mg/kg soluble PHCCC or PHCCC NPs at (A) five day or (F) three day intervals. Disease pathology was assessed daily using the clinical scale described in the methods. (B) Mean clinical score time course for mice treated using the regimen in (A). (C) Individual clinical scores of mice shown in (B) on days 10 and 15. (D) Incidence of disease (EAE score > 0) for the mice in (B). (E) Maximum mean score observed during studies using the regimen in (A). (G) Mean clinical score time course for mice treated using the regimen in (F). (H) Individual clinical scores of mice shown in (G) on days 10 and 15. (I) Incidence of disease (EAE score > 0) for the mice in (G). (J) Maximum mean score observed during studies using the regimen in (F). Studies were conducted with groups of 6 mice. Unpaired T tests were used to compare between groups at each study day. An alpha value of 0.05 was used to determine significance (*).

During in vitro studies, PHCCC NPs exhibited several favorable properties compared with soluble drug. First, PHCCC could be solubilized and slowly released from NPs without need of solvents or other vehicles (e.g., sesame oil). PHCCC delivered in particle form was 36-fold less toxic, with equivalent doses in soluble exhibiting high levels of toxicity compared to PHCCC NPs (Fig. 1F). Interestingly, PHCCC toxicity was almost completely eliminated when delivered in NP format, approaching the levels measured in unstimulated controls. This observation was true even at the higher concentrations required for PHCCC NPs to match the effectiveness of soluble PHCCC (Fig. 1F). Although toxicity was absent when cells were treated with PHCCC NPs, clear effects on DCs (e.g., surface markers, cytokine profiles) and T cells were observed, indicating a modulatory function rather than toxicity or cell death.

The immunomodulatory effects of soluble PHCCC on DCs were maintained when PHCCC was delivered in NPs, though higher concentrations had to be delivered to achieve the same level of change in cytokine profiles and activation marker expression. This observation may result from the controlled release of PHCCC from NPs. Soluble PHCCC delivery results in immediate availability of all drug, while PHCCC is released from NPs over time (Fig. 1C). DC activation studies lasted 18 h, and while release studies show that 75% of drug was released over this interval under sink conditions, without the DMSO vehicle used in soluble PHCCC treatments, drug release from particles likely achieved a much lower effective solution concentration of free drug in cell culture wells compared to the solution concentration in wells treated with soluble formulations containing DMSO. This idea may also explain why lower concentrations of PHCCC NPs were more effective than soluble drug in promoting T_{REGS}, reducing IFNγ, and limiting T cell proliferation during co-culture studies that continued for 96 h. For example, 400 μM PHCCC NP had a similar effect to 40 μM soluble PHCCC on reducing DC activation (Fig. 4A–C), while 50 μM PHCCC NP caused a larger reduction in T cell proliferation compared to 40 μM soluble PHCCC (Fig. 5A and B). Soluble drug may be exhausted or degraded over this interval, whereas drug in particles may be more stable. The greater time for metabolism of drug in solution could also allow dissolution of more drug as it is released from particles over this interval, or of drug that has locally precipitated.

Since fluorescent analogs of PHCCC have not been reported, we studied uptake using NPs loaded with a fluorescent lipophilic dye as a model cargo. Our results demonstrate that these NPs are readily internalized by DCs (Fig. 1D and E). Thus, in addition to reduced toxicity, NP-mediated delivery may provide a simple method of targeting PHCCC to DCs residing in lymph nodes or spleens since antigen presenting cells are specialized to internalize particulate materials over soluble molecules [18,19]. This possibility is important because DCs present autoantigens to T cells in lymphoid organs [6–8]. Thus, to polarize T cell function and ameliorate autoimmune responses, it may be beneficial for immunomodulatory drugs acting on DCs to reach the lymphoid organs and persist at sufficient concentrations in these tissues during (self) antigen presentation. Further, soluble delivery results in systemic exposure of drug, while NPs reach lymph nodes through passive drainage and through trafficking by DCs after NP uptake. Using PHCCC NPs that release PHCCC over an extended time could help target LNs and avoid systemic exposure while avoiding continual dosing of soluble drug.

Although PLGA has traditionally been seen as immunologically inert, recent studies have demonstrated that PLGA can activate DCs and inflammasome pathways, amplify immune responses to toll-like receptor agonists, and cause secretion of inflammatory cytokines [30,31]. Thus, empty NP controls were included in all experiments in order to isolate any intrinsic polymer effects from the encapsulated PHCCC. The highest masses of empty NPs – correlating to the lowest drug to polymer ratios – generally had a slight suppressive effect on cytokine secretion (Fig. 3), but minimal effects on DC activation (Fig. 4) and T cell studies (Fig. 5). Interestingly, other reports demonstrate a decrease in the expression of DC activation markers when DCs are treated with PLGA particles for 48 h before stimulation with LPS [32]. From a physicochemical standpoint, the slight effects of empty particles observed in our experiments at high concentrations may be driven by acidification of the media from lactic acid byproducts as PLGA degrades [33].

During adaptive immune response, IL-6 and IL-12 drive proinflammatory function, secreted by DCs to promote T_H17 and T_H1 cells, respectively [34]. IL-10 is a polyfunctional cytokine, but often serves as a negative regulator to restrain DC function. Although IL-10 production is a goal of many tolerogenic therapies, PHCCC has been shown to

decrease IL-10 production in response to LPS stimulation. The proposed mechanism for this process is drug-mediated reduction of the cAMP triggered by LPS, resulting in a shift away from cytokines that drive T_H17 cells and toward cytokines that promote T_{REG} and T_H1 [10]. Therefore PHCCC is a modulator, and not a strict immunosuppressive agent. We observed these effects through a decrease in IL-6 and IL-10 secretion compared to untreated DCs stimulated with LPS (Figs. 2 and 3), but did not observe any differences in IL-12 secretion (data not shown). Interestingly, after LPS stimulation, IL-10 secretion was delayed compared with inflammatory cytokines (Figs. 2D–F and 3D–F), in agreement with the natural time course for regulation during which IL-10 supports return of immune function to basal homeostatic levels following inflammation or infection events [34].

The effects of PHCCC on DCs described above have an important impact on T cell differentiation and function during autoimmunity. For example, during EAE and MS, disease is driven by subsets of $CD4^+$ helper T cells, but it is unclear whether T_H17 or T_H1 cells induce more severe pathology [34]. The Di Marco group has shown that protective effects of PHCCC treatment on EAE coincide with a shift away from T_H17 cells and toward not only T_{REG}, but also IFNγ-producing T_H1 cells [10]. Our co-culture studies revealed that treatment with PHCCC NPs shifted T cells away from T_H17 and toward T_{REG} phenotypes, while decreasing IFNγ (Fig. 5). Thus, although we did not observe an increase in T_H1 function (e.g., increased IFNγ), decreased levels of IFNγ associated with delivery of PHCCC NPs could be beneficial in reducing the activity of autoreactive T cells during EAE or other autoimmune diseases [3].

In recent studies, soluble PHCCC protected mice from EAE when injected daily in sesame oil as a vehicle. However, symptoms rapidly returned in less than 24 h when treatment was stopped for even a single day [10]. In our studies, PHCCC NPs delivered every 5 days had no effect on clinical score compared to mice treated with empty NPs or soluble PHCCC (Fig. 6A–E). However, when PHCCC NPs were administered every three days, these particles delayed the onset of EAE and reduced the severity of disease compared with soluble drug (Fig. 6F–J) or empty NPs (Fig. S3). From a pharmacokinetic perspective, a likely explanation is that NPs do not provide a drug concentration in the therapeutic window with 5 day intervals, which based on the release studies (Fig. 1C), appear to be during a time frame over which the drug release rate is negligible. While release studies indicated ~75% of drug was released over 8 h, we observed a significant reduction in disease progression when mice were treated with PHCCC NPs at three day intervals, but not when soluble treatments were administered at this frequency. These effects may have been supported by the slower, but sustained release from NPs that occurred over 8 to 72 h (Fig. 1c). Owing to the sparing solubility (10 μg/mL), local precipitation of PHCCC due to non-sink conditions in injected animals may also have slowed the release rate. Taken together, these findings highlight the potential of controlled release to improve the delivery of immunomodulatory signals that modulate DC metabolism to promote tolerance. These experiments also underscore the need to develop controlled release formulations that achieve longer-term release to provide greater reductions in the frequency of injection.

Although treatment with PHCCC NPs successfully delayed the onset of neurological symptoms, autoimmunity eventually progressed to an incidence of 100%. This was evident through similar mean clinical scores in both PHCCC NP and soluble groups at the end of the experiment. These results are consistent with findings from the Di Marco group indicating that PHCCC does not reverse established disease even when soluble PHCCC is administered daily starting one day after the appearance of neurological symptoms [19]. Thus, controlled release from PHCCC NPs may initially be sufficient to delay symptoms, but as the concentration of PHCCC wanes over the 3 day interval, myelin-reactive events (e.g., T cell expansion) may increase to cause neurodegeneration that is not reversed even when another dose of PHCCC NPs is administered. This idea further highlights the opportunity to use controlled release to enhance metabolic control over DC and T cell function by exploring polymeric materials that provide longer term or higher levels of release, or by incorporating other components such as DC targeting molecules or more potent mGluR4 enhancers.

5. Conclusion

In this study we utilized an established nanoprecipitation platform to test the new idea that controlled delivery of a glutamate receptor enhancer could alter immune cell function to improve autoimmune therapy. PHCCC NPs exhibited greatly reduced toxicity, while maintaining the immunomodulatory effects of soluble PHCCC on DCs and T cells in vitro. Treatment of mice with PHCCC NPs delayed disease and decreased severity compared to mice treated with soluble PHCCC. More broadly, this report demonstrates that controlled delivery of metabolic modulators can be exploited to direct DC function for promoting tolerance. This idea could contribute to new therapeutic options for autoimmunity or inflammatory disease.

Acknowledgments

This work was supported in part by NSF CAREER Award # 1351688, the National Multiple Sclerosis Society # PP2103, and the Pharmaceutics division of the PhRMA Foundation # 13071672. CMJ is a Damon Runyon-Rachleff Innovator supported by the Damon Runyon Foundation (# DDR3415), a Young Investigator supported by the Alliance for Cancer Gene Therapy (# 15051543), and a Young Investigator support by the Melanoma Research Alliance (# 348963). LHT is a NSF Graduate Research Fellow supported by grant # DGE1322106.

Appendix A. Supplementary data

Supplementary data to this article can be found online at http://dx.doi.org/10.1016/j.jconrel.2015.05.277.

References

[1] F. Danhier, E. Ansorena, J.M. Silva, R. Coco, A. Le Breton, V. Preat, PLGA-based nanoparticles: an overview of biomedical applications, J. Control. Release 161 (2) (2012) 505–522 (PubMed PMID: WOS:000305790300035. English).
[2] J.I. Andorko, K.L. Hess, C.M. Jewell, Harnessing biomaterials to engineer the lymph node microenvironment for immunity or tolerance, AAPS J. 17 (2014) 323–338.
[3] D.J. Irvine, M.A. Swartz, G.L. Szeto, Engineering synthetic vaccines using cues from natural immunity, Nat. Mater. 12 (11) (2013) 978–990 (PubMed PMID: 24150416. Pubmed Central PMCID: 3928825).
[4] A. Lutterotti, S. Yousef, A. Sputtek, K.H. Sturner, J.P. Stellmann, P. Breiden, et al., Antigen-specific tolerance by autologous myelin peptide-coupled cells: a phase 1 trial in multiple sclerosis, Sci. Transl. Med. 5 (188) (2013) 188ra75 (PubMed PMID: 23740901. Pubmed Central PMCID: 3973034).
[5] L. Steinman, Multiple sclerosis: a coordinated immunological attack against myelin in the central nervous system, Cell 85 (3) (1996) 299–302 (PubMed PMID: 8616884).
[6] H.F. McFarland, R. Martin, Multiple sclerosis: a complicated picture of autoimmunity, Nat. Immunol. 8 (9) (2007) 913–919 (PubMed PMID: 17712344).
[7] M. Comabella, S.J. Khoury, Immunopathogenesis of multiple sclerosis, Clin. Immunol. 142 (1) (2012) 2–8 (PubMed PMID: WOS:000299912600002. English).
[8] D. Pitt, P. Werner, C.S. Raine, Glutamate excitotoxicity in a model of multiple sclerosis, Nat. Med. 6 (1) (2000) 67–70 (PubMed PMID: WOS:000084583300037. English).
[9] B.D. Trapp, K.A. Nave, Multiple sclerosis: an immune or neurodegenerative disorder? Annu. Rev. Neurosci. 31 (2008) 247–269 (PubMed PMID: WOS:000257992200011. English).
[10] L. Peferoen, M. Kipp, P. van der Valk, J.M. van Noort, S. Amor, Oligodendrocyte-microglia cross-talk in the central nervous system, Immunology 141 (3) (2014) 302–313 (PubMed PMID: WOS:000330811600003. English).
[11] S.F. Spampinato, S. Merlo, M. Chisari, F. Nicoletti, M.A. Sortino, Glial metabotropic glutamate receptor-4 increases maturation and survival of oligodendrocytes, Front. Cell. Neurosci. 8 (2014) 462 (PubMed PMID: 25642169. Pubmed Central PMCID: 4294134).
[12] M. Maj, V. Bruno, Z. Dragic, R. Yamamoto, G. Battaglia, W. Inderbitzin, et al., (−)-PHCCC, a positive allosteric modulator of mGluR4: characterization, mechanism of action, and neuroprotection, Neuropharmacology 45 (7) (2003) 895–906 (PubMed PMID: WOS:000186378800002. English).

[13] M. Julio-Pieper, P.J. Flor, T.G. Dinan, J.F. Cryan, Exciting times beyond the brain: metabotropic glutamate receptors in peripheral and non-neural tissues, Pharmacol. Rev. 63 (1) (2011) 35–58 (PubMed PMID: WOS:000287356800002. English).
[14] R.M. Steinman, H. Hemmi, Dendritic cells: translating innate to adaptive immunity, Curr. Top. Microbiol. 311 (2006) 17–58 (PubMed PMID: WOS:000241815600002. English).
[15] R.M. Steinman, D. Hawiger, M.C. Nussenzweig, Tolerogenic dendritic cells, Annu. Rev. Immunol. 21 (2003) 685–711 (PubMed PMID: WOS:000182523500021. English).
[16] A.E. Morelli, A.W. Thomson, Tolerogenic dendritic cells and the quest for transplant tolerance, Nat. Rev. Immunol. 7 (8) (2007) 610–621 (PubMed PMID: WOS:000248394100013. English).
[17] A. Lutterotti, R. Martin, Antigen-specific tolerization approaches in multiple sclerosis, Expert Opin. Investig. Drugs 23 (1) (2014) 9–20 (PubMed PMID: WOS:000328110700002. English).
[18] R. Pacheco, H. Oliva, J.M. Martinez-Navio, N. Climent, F. Ciruela, J.M. Gatell, et al., Glutamate released by dendritic cells as a novel modulator of T cell activation, J. Immunol. 177 (10) (2006) 6695–6704 (PubMed PMID: WOS:000242009700017. English).
[19] F. Fallarino, C. Volpi, F. Fazio, S. Notartomaso, C. Vacca, C. Busceti, et al., Metabotropic glutamate receptor-4 modulates adaptive immunity and restrains neuroinflammation, Nat. Med. 16 (8) (2010) 897-U94 (PubMed PMID: WOS:000280649200029. English).
[20] F. Fazio, C. Zappulla, S. Notartomaso, C. Busceti, A. Bessede, P. Scarselli, et al., Cinnabarinic acid, an endogenous agonist of type-4 metabotropic glutamate receptor, suppresses experimental autoimmune encephalomyelitis in mice, Neuropharmacology 81 (2014) 237–243 (PubMed PMID: WOS:000335632400025. English).
[21] R.S. Lopez-Diego, H.L. Weiner, Novel therapeutic strategies for multiple sclerosis — a multifaceted adversary, Nat. Rev. Drug Discov. 7 (11) (2008) 909–925 (PubMed PMID: WOS:000260532400022. English).
[22] C.M. Niswender, K.A. Johnson, C.D. Weaver, C.K. Jones, Z.X. Xiang, Q.W. Luo, et al., Discovery, characterization, and antiparkinsonian effect of novel positive allosteric modulators of metabotropic glutamate receptor 4, Mol. Pharmacol. 74 (5) (2008) 1345–1358 (PubMed PMID: WOS:000260197300017. English).
[23] E. Bettelli, M. Pagany, H.L. Weiner, C. Linington, R.A. Sobel, A.K. Kuchroo, Myelin oligodendrocyte glycoprotein-specific T cell receptor transgenic mice develop spontaneous autoimmune optic neuritis, J. Exp. Med. 197 (9) (2003) 1073–1081 (PubMed PMID: WOS:000182752000002. English).
[24] I. Mendel, N. Kerlero de Rosbo, A. Ben-Nun, A myelin oligodendrocyte glycoprotein peptide induces typical chronic experimental autoimmune encephalomyelitis in H-2b mice: fine specificity and T cell receptor V beta expression of encephalitogenic T cells, Eur. J. Immunol. 25 (7) (1995) 1951–1959 (PubMed PMID: 7621871).
[25] T. Korn, J. Reddy, W. Gao, E. Bettelli, A. Awasthi, T.R. Petersen, et al., Myelin-specific regulatory T cells accumulate in the CNS but fail to control autoimmune inflammation, Nat. Med. 13 (4) (2007) 423–431 (PubMed PMID: 17384649. Pubmed Central PMCID: 3427780).
[26] M. Look, E. Stern, Q.A. Wang, L.D. DiPlacido, M. Kashgarian, J. Craft, et al., Nanogel-based delivery of mycophenolic acid ameliorates systemic lupus erythematosus in mice, J. Clin. Invest. 123 (4) (2013) 1741–1749 (PubMed PMID: WOS:000317021800033. English).
[27] S. Jhunjhunwala, G. Raimondi, A.W. Thomson, S.R. Little, Delivery of rapamycin to dendritic cells using degradable microparticles, J. Control. Release 133 (3) (2009) 191–197 (PubMed PMID: 19000726. Pubmed Central PMCID: 2925512).
[28] R.A. Maldonado, R.A. LaMothe, J.D. Ferrari, A.H. Zhang, R.J. Rossi, P.N. Kolte, et al., Polymeric synthetic nanoparticles for the induction of antigen-specific immunological tolerance, Proc. Natl. Acad. Sci. U. S. A. 112 (2) (2015) E156–E165 (PubMed PMID: WOS:000347732300010. English).
[29] A. Yeste, M. Nadeau, E.J. Burns, H.L. Weiner, F.J. Quintana, Nanoparticle-mediated codelivery of myelin antigen and a tolerogenic small molecule suppresses experimental autoimmune encephalomyelitis, Proc. Natl. Acad. Sci. U. S. A. 109 (28) (2012) 11270–11275 (PubMed PMID: WOS:000306642100052. English).
[30] F.A. Sharp, D. Ruane, B. Claass, E. Creagh, J. Harris, P. Malyala, et al., Uptake of particulate vaccine adjuvants by dendritic cells activates the NALP3 inflammasome, Proc. Natl. Acad. Sci. U. S. A. 106 (3) (2009) 870–875 (PubMed PMID: WOS:000262809700037. English).
[31] J. Park, J.E. Babensee, Differential functional effects of biomaterials on dendritic cell maturation, Acta Biomater. 8 (10) (2012) 3606–3617 (PubMed PMID: WOS:000309301400007. English).
[32] J.S. Lewis, C. Roche, Y. Zhang, T.M. Brusko, C.H. Wasserfall, M. Atkinson, et al., Combinatorial delivery of immunosuppressive factors to dendritic cells using dual-sized microspheres, J. Mater. Chem. B 2 (17) (2014) 2562–2574 (PubMed PMID: WOS:000334121500023. English).
[33] E. Gottfried, L.A. Kunz-Schughart, S. Ebner, W. Mueller-Klieser, S. Hoves, R. Andreesen, et al., Tumor-derived lactic acid modulates dendritic cell activation and antigen expression, Blood 107 (5) (2006) 2013–2021 (PubMed PMID: WOS:000235632700046. English).
[34] R. Samarasinghe, P. Tailor, T. Tamura, T. Kaisho, S. Akira, K. Ozato, Induction of an anti-inflammatory cytokine, IL-10, in dendritic cells after toll-like receptor signaling, J. Interf. Cytokine Res. 26 (12) (2006) 893–900 (PubMed PMID: WOS:000243076600006. English).